Available online at www.sciencedirect.com
SCIENCE DIRECT®
Cement & Concrete Composites 26 (2004) 947–956
Cement & Concrete Composites
www.elsevier.com/locate/cemconcomp

Revisiting the microstructure of hydrated tricalcium silicate—a comparison to Portland cement

Knut O. Kjellsen [a,*], Harald Justnes [b]

[a] Norcem AS, R&D Department, N-3950 Brevik, Norway
[b] SINTEF, Civil and Environmental Engineering, N-7465 Trondheim, Norway

Abstract

The microstructures of 0.40 w/s-ratio pastes of tricalcium silicate (C_3S), alite and Portland cement have been studied at the hydration times 24 h and 1 month. A field-emission SEM (FE-SEM) was used to obtain high-resolution backscattered electron images. Comparison revealed no microstructural differences between C_3S and alite, but there were considerable differences in microstructure between C_3S and Portland cement pastes. The microstructure of the C_3S paste was simpler than that of the Portland cement, and could be described by a few characteristic features. Distribution of the reaction products differed substantially in the two systems. While hollow shells (Hadley grains) were a prominent feature of the Portland cement paste, their occurrence was more limited in the C_3S and alite pastes. Hollow shells were restricted to grains smaller than about 5 μm in the C_3S and alite pastes, and gapped hollow shells were not a common feature.

Keywords: Tricalcium silicate; C_3S; Alite; Portland cement; Microstructure; FE-SEM; SEM

1. Introduction

Alite, the impure form of tricalcium silicate (C_3S), typically constitutes around 60% of a modern Portland cement. The major constituents of hydrated Portland cement are calcium silicate hydrate (C–S–H) and calcium hydroxide (CH), of which both are produced mainly from the reaction between alite and water. Portland cement and C_3S are similar in their setting and hardening characteristics. Neither alite nor C_3S are industrial products as Portland cement is. However, as alite is the most important phase of cement and is much simpler, alite or C_3S has been commonly prepared in the laboratory and used as a model system for the hydration of Portland cement.

SEM studies of hydrated alite or C_3S dates somewhat back in time, when secondary electrons were used as source of imaging for characterizing fractured surfaces [1–4]. We are only aware of one study utilizing backscattered electrons to characterize flat polished specimens of pure C_3S or alite pastes [5]. Some contradictory information of the microstructure of hydrated alite and C_3S seems to exist, concerning for example the distribution of CH, and in particular as to the question of Hadley grains. In this paper we discuss these questions, and also the similarities and dissimilarities in the microstructure of C_3S and Portland cement pastes in a broader sense.

We adopted a field-emission SEM to obtain high-resolution backscattered electron images of polished specimens. The FE-SEM possesses potentially improved resolution capability over the standard SEM. It was possible to obtain backscattered electron images of reasonably good resolution at magnifications up to about 20,000×, or nearly 10 times that obtainable from conventional SEM [6]. The level of detail obtained in low-resolution transmission electron microscopy (TEM) [7–11] is thus approached, allowing for comparison of microstructural features by the two techniques.

2. Experimental

2.1. Materials and specimen preparation

Triclinic tricalcium silicate (C_3S, or $3CaO \cdot SiO_2$), alite, and a Portland cement were used in this study. The

* Corresponding author. Tel.: +47-35-57-2357; fax: +47-35-57-0400.
E-mail address: knut.kjellsen@norcem.no (K.O. Kjellsen).

0958-9465/$ - see front matter © 2004 Elsevier Ltd. All rights reserved.
doi:10.1016/j.cemconcomp.2004.02.030

Table 1
Characteristics of the materials

	C_3S	Alite	Cement
SiO_2 (%)	26.2	26.0	22.2
CaO (%)	73.6	72.8	64.9
Al_2O_3 (%)	0.29	0.83	3.4
Fe_2O_3 (%)	–	–	4.8
MgO (%)	0.10	0.45	0.91
SO_3 (%)	–	–	2.0
K_2O (%)	–	–	0.56
Na_2O (%)	–	–	0.04
Free lime (%)	0.31	0.37	0.70
Loss-on-ignition (%)	–	–	0.63%
Specific surface area (Blaine) (m^2/kg)	332	334	302
Specific weight (kg/m^3)	3110	3110	3220

Percentage by mass.

alite was a monoclinic C_3S, stabilized by aluminum and magnesia. The C_3S and alite were both supplied by Dr P B West, Construction Technology Laboratories, Illinois. The Portland cement was a Swedish low-alkali sulfate-resistant Portland cement (which corresponds to ASTM Type V). The characteristics of the three materials are provided in Table 1. Pastes were made of deionized water and the anhydrous materials at a water/solid ratio of 0.40. The C_3S and alite pastes were mixed by hand. After the pastes were mixed they were cast into small polyethylene bottles and slowly rotated to avoid separation. The cement paste was produced in another project a few years earlier. The cement paste was more rigorously mixed than the C_3S and alite pastes, and it contained a superplasticizer (Mighty 150) at a dosage level of 0.2% (dry weight) by weight of cement. Details of the production of the cement paste specimens are given in [12,13]. All specimens were stored in sealed containers, to prevent moisture exchange and carbonation. Mixing and storage took place at 20 °C.

Hydration was stopped at the predetermined ages of 24 h and of 1 month. Thin paste slices a few mm wide were cut off from the larger specimens by a precision diamond splitting wheel. The paste fragments were submerged in liquid nitrogen to stop hydration. They were later freeze-dried, except that for practical reasons, the 1-month old C_3S and alite pastes were oven dried at 105 °C after being submerged in ethanol for a few days. All specimens were epoxy-impregnated and polished flat for examination in the SEM and FE-SEM. Details of the preparation of the polished specimens are given elsewhere [14].

2.2. Method

Micrographs were obtained in a conventional Jeol 840A SEM, and in a Hitachi S-4300 SE field-emission SEM. Both microscopes were operated at an accelerating voltage of 10 kV. Several sections of each specimen were always examined, and all images presented are representative of the various specimens.

3. Results and discussion

3.1. Distribution of CH

Fig. 1 depicts a backscattered electron SEM image of the C_3S paste hydrated for 24 h, taken in a conventional SEM. CH grows from only a few centers, and precipitates as very large deposits in the C_3S paste (an example is outlined in Fig. 1). On further hydration between 24 h and 28 days, most of the CH growth continues in the vicinity of previously formed CH assemblages. In other words, the large CH masses grow larger on continued hydration and tend to grow into each other. This can be observed in Fig. 2, which shows a backscattered electron

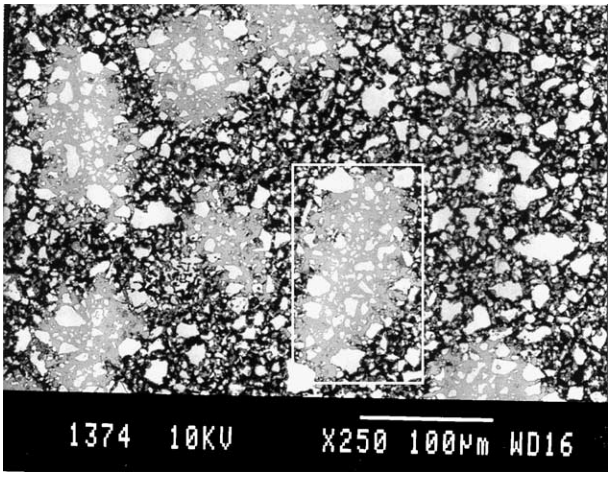

Fig. 1. Backscattered electron image (SEM) of the C_3S paste hydrated for 24 h. Magnification: 250×.

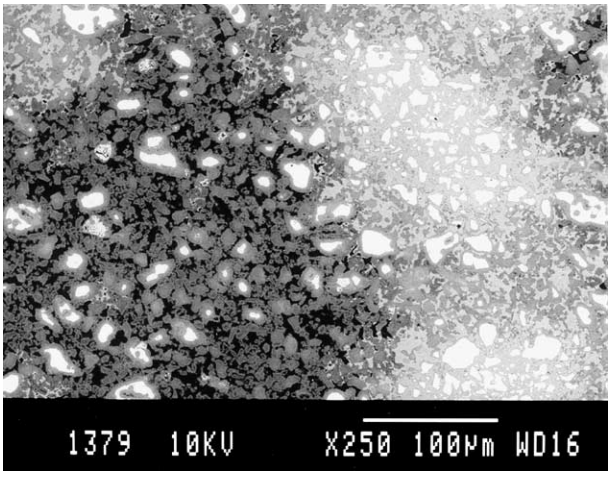

Fig. 2. Backscattered electron image (SEM) of the alite paste hydrated for 1 month. Magnification: 250×.

image of the alite paste hydrated for 1 month. Intergrown masses of CH are here seen to the right in the micrograph. CH appears to have totally filled up the available water-filled pore space in large areas after 1 month. The capillary pore space (i.e. the residue of the originally water-filled space not filled with hydrates [15]) outside the areas containing massive CH is practically empty of visible CH as seen from the left portion of Fig. 2. Pores are seen as black in backscattered electron images. At 24 h the largest CH deposits were larger than 100 μm across. After 1 month the inter-grown CH assemblages had often grown to several hundred μm across. CH often grew around and completely engulfed some C_3S particles (see Fig. 2). The very large CH deposits seen here in both the C_3S and alite pastes have been observed previously in triclinic C_3S paste [1,16–18]. It appears, however, that these large CH agglomerates did not form in the alite paste studied by Jennings and Parrott [5]. We have not observed this texture in hand mixed cement paste before, and consequently do not think they are due to the effect of mixing.

The very large and concentrated masses of CH seen in the C_3S and alite pastes are different from that seen in Portland cement. In cement systems, CH forms as comparatively much more finely dispersed particles throughout the microstructure. The visible pore space appears much more congested and complex in the Portland cement paste than in the C_3S and alite pastes, as will be discussed later. The shapes of the CH particles appear also to be more complex and diversified in cement paste. The high degree of irregularity and geometrical complexity of many CH particles in Portland cement system [19] reflect the tortuous character of the capillary pore space (as seen in Fig. 3). The thin platy CH crystals frequently seen in Portland cement systems were not found in the C_3S or alite pastes in this work.

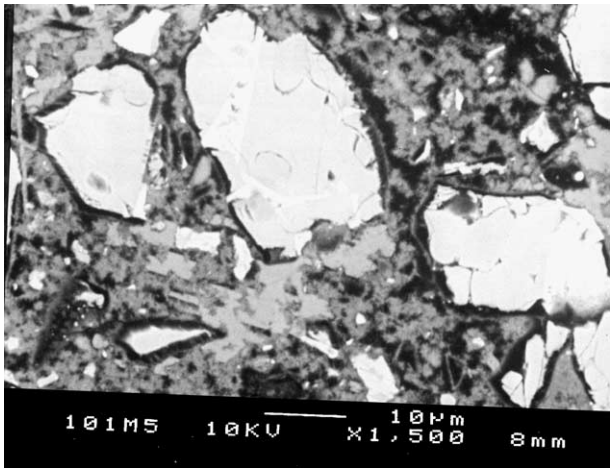

Fig. 3. Backscattered electron image (SEM) of the Portland cement paste hydrated for 24 h. Magnification: 1500×.

The increased geometrical constraints developed in Portland cement pastes in the regions where CH can grow can be one reason for the higher number of CH particles. It is also likely that difference in the solubility of CH at different pH levels has influenced the CH morphology. The pH in Portland cement paste is expected to be much higher than that in C_3S paste, due to the presence of alkalis in the former system. This implies reduced CH solubility due to the common ion effect, and should promote nucleation of CH. For example, Berger and McGregor [17] observed that the number of CH crystals in C_3S paste increased with increasing temperature. They associated the increased number of CH crystals to the lower CH solubility at higher temperature. Boyer and Berger [18] found that by rapidly increasing the degree of solution supersaturation with respect to CH through sudden temperature increase, many more but much smaller particles of CH formed in C_3S systems.

3.2. Hadley grains in C_3S and alite pastes

When Portland cement grains decrease in size upon hydration, Taplin [20] predicted that reaction products would form simultaneously inside ('inner' products) and outside ('outer' products) the original cement grain boundaries. Direct observations of the microstructure [6,12,21–27] of Portland cement systems support another possibility; namely that stable inner products may not always form. Instead, a void of up to some micrometers wide is established between a layer of product and the receding cement core. As the cement core continues to dissolve a progressively larger void space may develop within the shell of product. Smaller cement grains may undergo rapid and complete hollow-shell hydration, and leave empty hydration shells. Fig. 3 reveals examples of the distinct hollow-shell separations between cement grains (bright particles) and the rims of the surrounding hydration product (gray) so commonly observed in Portland cement systems.

It has been stated that hollow shells or Hadley grains, as they also have been named after the man who first discovered them (David W Hadley [21]), seem not to form in C_3S paste [24,28,29]. Of these authors, Pratt and Ghose [24] and Taylor et al. [28] presented no experimental results to support this view. Scrivener and Pratt [29] studied a mixture of monomineralic grains of C_3S and C_3A (plus hemihydrate) and found close contact between the C_3S grains and product at 1 day. However, they found huge separations between C_3A grains and their hydration shells. Scrivener and Pratt associated the formation of Hadley grains in cement paste to the formation of ettringite on the layer of C–S–H product forming on alite grains. On the other hand, Hadley et al. [27] reported hollow-shell formation to some limited extent in alite paste alone. They made their study on

3-day old specimens, and the occurrence of hollow shells became more common in alite-gypsum and alite-gypsum-C_3A systems. Ettringite formation did not seem to be a necessary feature for the formation of hollow-shell grains. Hadley and co-workers used secondary electrons to study surfaces exposed by fracture. As they point out, with this technique detection of hollow-shell hydration grains is very much a hit-and-miss affair. One can only get a vague impression of how common hollow shells are with this technique, as not all hollow shells will be fractured and expose their interior.

Fig. 4 reveals a backscattered electron image of the alite paste hydrated for 24 h. The black continuous phase represents the capillary pore space. The image depict a part of the specimen were no visible CH has formed (cf. previous section). Thin layers of reaction product (C–S–H) have formed around the bright anhydrous alite particles. In agreement with the citations referred to and others, there seems to be contact between the anhydrous alite cores and the shell of C–S–H. However, there appear also to be a number of small completely empty hydration shells. A few examples are outlined. Images showing the small hydration shells in detail are difficult to obtain in a conventional SEM, due to poor resolution at magnifications much above that of Fig. 4. In contrast, Fig. 5 shows a FE-SEM backscattered electron image of the C_3S paste hydrated for 24 h at much higher magnification than Fig. 4. What appear to be two small hollow-hydration shells are seen to the left in the image. Their center seems hollowed, although a dimly textured phase of C–S–H appears to protrude towards their center. Such weakly defined C–S–H phases on the inside of the hydration shells were not always observed, and may not be typical. The character of the shells indicates they are remnants of small C_3S particles that have undergone hollow-shell hydration. These essentially hollow shells are without exceptions smaller than some 5 μm across. The apparent thickness of the shells is generally about 0.5 μm, as revealed from backscattered electron images. They seem to originate from C_3S particles smaller than about 5 μm across.

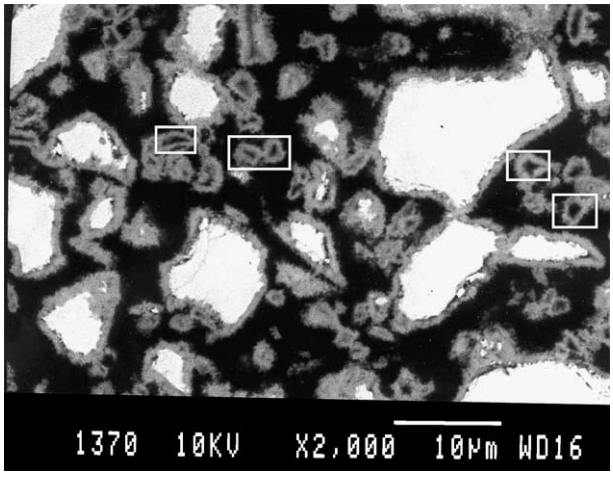

Fig. 4. Backscattered electron image (SEM) of the alite paste hydrated for 24 h. Magnification: 2000×.

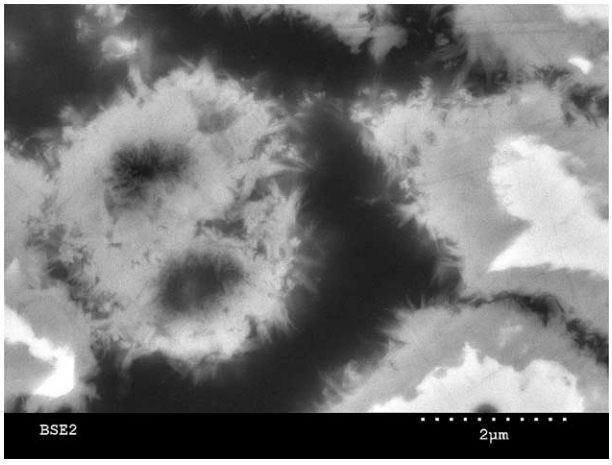

Fig. 5. Backscattered electron image (FE-SEM) of the C_3S paste hydrated for 24 h. Magnification: 15,000×.

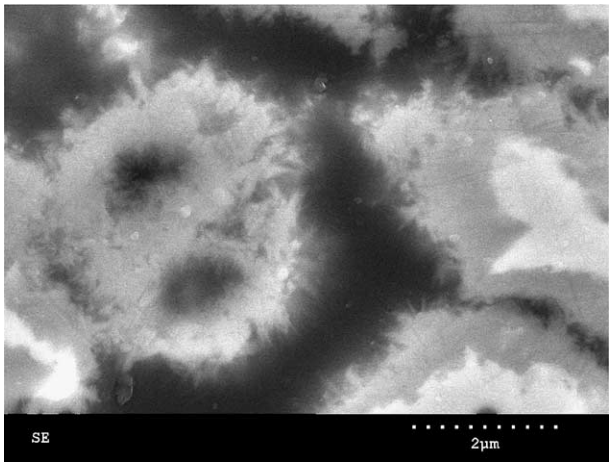

Fig. 6. FE-SEM image of the field from Fig. 5 obtained using a secondary electron detector.

Fig. 6 shows a secondary electron image of the section depicted in Fig. 5. The secondary electron image reveals essentially topographical information of the surface of the specimen. The surface appears very smooth, practically without scratches or any imperfections. All specimens were not this well prepared, but Fig. 5 demonstrates that it is possible to produce polished specimens well suited for high-magnification study. It is evident that epoxy has filled all visible pore spaces, including the hollow shells. As impregnation with resin takes place before grinding and polishing [14], it becomes clear that that the hollow shells are real and have not resulted from material being pulled out during

preparation. The hollow-shell features presented in this paper are all filled with epoxy resin.

Two high-magnification backscattered electron images of the Portland cement paste hydrated for 24 h are depicted in Figs. 7 and 8. Secondary electron images shown as Figs. 9 and 10 revealed effective epoxy impregnation and relatively smooth surfaces; the elemental contrast observed is likely due to backscattered electrons impinging on the secondary electron detector. Badly polished specimens do show the expected surface topography variations. An apparently empty hollow shell originating from complete hollow-shell hydration of a small cement grain is seen in Fig. 7. Fig. 8 depicts a partially hollow shell, with its anhydrous cement core being separated from the surrounding hydration product. As discussed in the beginning of this section, this type of hydration shell being separated from the cement grain is commonly observed in Portland cement systems during the first few days of hydration. At somewhat later ages the mode of hydration may change, and these intra-shell separations then often become filled with late-deposited reaction products. As previously indicated, such intra-shell gaps typical for Portland cement were never seen in the C_3S and alite pastes at the ages examined, where there was close contact between the anhydrous grains and the surrounding product layer in the larger, partly hydrated grains.

Hollow shells observed in the C_3S and alite pastes at 24 h (Figs. 4 and 5) apparently change character at later ages. Clearly defined hollow-shells became considerably fewer at 1 month, though a few were still seen virtually unchanged. In contrast, hydration shells of the same size filled with an interior product C–S–H were much more plentiful at 1 month than at 24 h. The gray tone of the interior product phase of such grains varied widely within grains and between grains at 1 month. An example is given in Fig. 11, which shows a high-magnification backscattered electron image of the C_3S

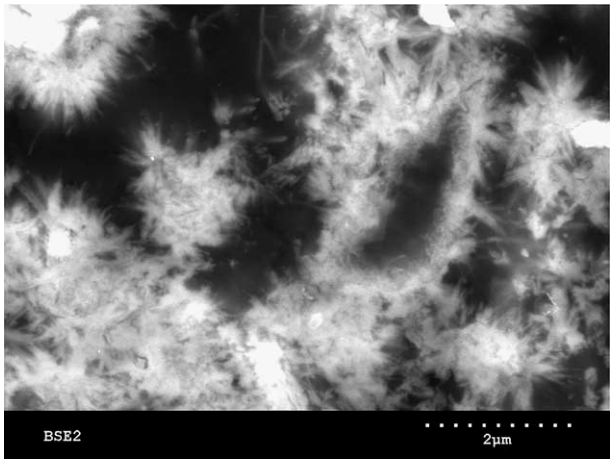

Fig. 7. Backscattered electron image (FE-SEM) of the cement paste hydrated for 24 h. Magnification: 15,000×.

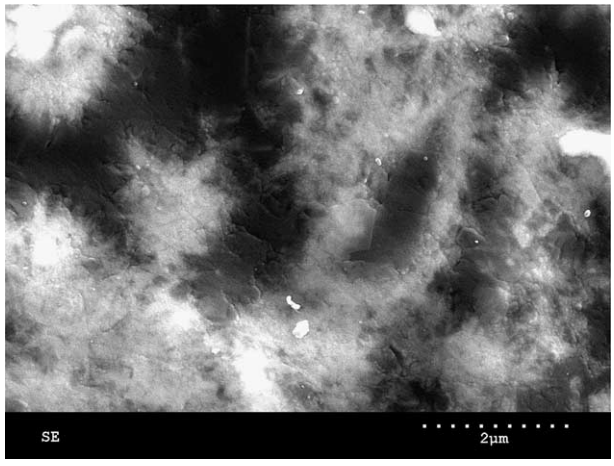

Fig. 9. FE-SEM image of the field from Fig. 7 obtained using a secondary electron detector.

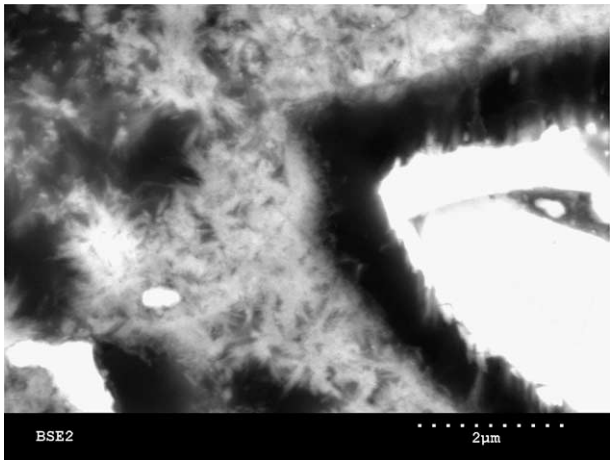

Fig. 8. Backscattered electron image (FE-SEM) of the cement paste hydrated for 24 h. Magnification: 15,000×.

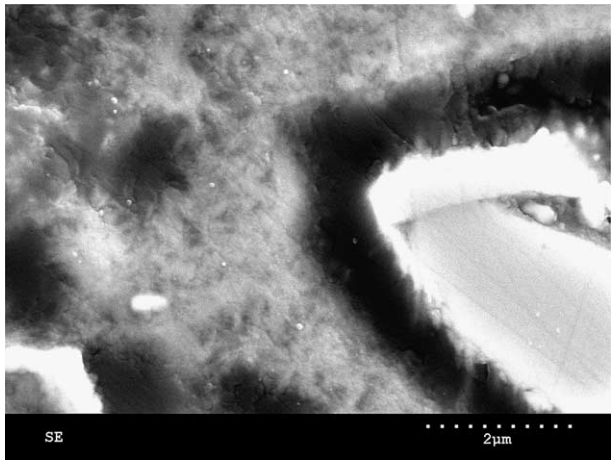

Fig. 10. FE-SEM image of the field from Fig. 8 obtained using a secondary electron detector.

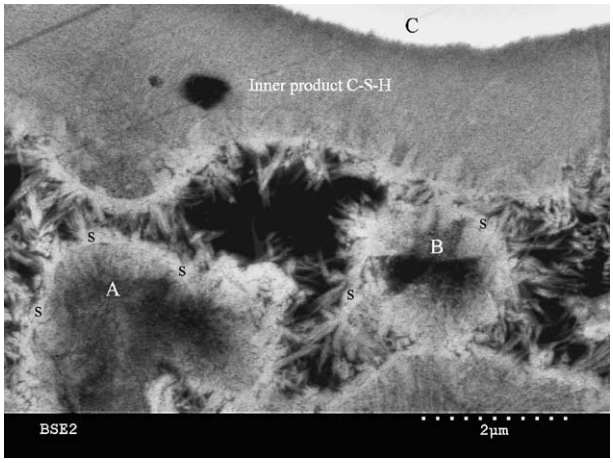

Fig. 11. Backscattered electron image (FE-SEM) of the C_3S paste hydrated for 1 month. Magnification: 15,000×. A and B, hydrated grains; s, shell of C–S–H; C, anhydrous C_3S.

paste hydrated for 1 month. Two small grains (marked A and B in Fig. 11) are composed of a relatively bright shell of C–S–H (denoted as s), while a considerably darker gray interior C–S–H phase is observed inside the shells. The inner product C–S–H phase located in close contact to the anhydrous C_3S core (denoted C) at the top of the micrograph is considerably brighter than much of the interior product phase of the two small grains (A and B). The bright inner C–S–H phases had always a fine-scale morphology without resolvable porosity. All remnant C_3S cores were surrounded by this bright inner C–S–H phase, which revealed only small variations in physical appearance. Porosity is visible in the darker gray interior phases of the small grains located in the lower part of the image (A and B). Many small grains had C–S–H interior product with gray level in between the varieties shown in Fig. 11.

From transmission electron micrographs Richardson and Groves [30] observed what they termed 'small fully hydrated grains (<5 μm)' in pastes of Portland cement, as well as in pastes of C_3S. They reported that the interior of these small hydrated grains contained an unusually coarse foil-like C–S–H containing substantial porosity, and that they were surrounded by a zone of relatively dense C–S–H. The observations of Richardson and Groves were of specimens that had hydrated a few months, but the small grains of either C_3S or cement in their two types of specimens must have reacted fully during the early course of hydration. As discussed here, many of the small hollow shells we observed at 24 h changed character at later ages and apparently became deposited with a C–S–H phase of highly variable porosity. We consider that the small grains with darker gray (porous) interior product we have observed by FE-SEM (e.g. Fig. 11) probably are the same features as the small fully hydrated grains with the porous interior phase found by Richardson and Groves [30]. The coarse foil-like porous C–S–H they observed in their ion-thinned specimens with TEM probably takes a porous and dimly textured appearance in the SEM.

Richardson [10,11] later argued that low-density C–S–H within the hydration shells might appear dark in SEM backscattered electron images. It is clear that very porous phases of C–S–H can be made invisible in backscattered electron images by unfortunate settings of contrast and brightness. To help reduce this problem we used a relatively low contrast setting in many images. This reduced the span of gray levels, making low-density phases more visible. We found that reducing the contrast from a relatively high level while maintaining proper adjustment of brightness, made several apparently empty hydration shells to reveal the presence of interior C–S–H. Other shells did not change character upon these adjustments. With the contrast and brightness settings adopted, we consider that the images presented show appropriate elemental contrast, and the center of the hollow shells presented are in fact largely hollow.

Whether hollow-shell grains are completely hollow or contain a very porous product does not change the fact that deposition of stable hydrates within the boundaries of the original cement grain is in either case highly restricted. Hydrates have room to form inside the hydration shells when the anhydrous grain dissolves, but prefer to form stable products outside, leaving a completely empty void or an inner product phase with substantial porosity. It is also apparent that other empty shells are established early in the hydration process, but becomes fully or partly filled with products later. The question as whether hollow-shell grains have to be completely hollow, to become qualified for the designation was briefly discussed by Hadley et al. [27]. The phrasing 'completely' may be misleading, as reaction products appear to have formed to some extent within the original cement grain peripheries in most hollow-shell grains.

3.3. Distribution of C–S–H at 24 h

The microstructure of the C_3S and alite pastes appear simpler and more ordered than that of the cement paste (cf. Figs. 3 and 4). The capillary pore space in the C_3S and alite pastes is much more spacious compared to that of the Portland cement paste. Fig. 3 is representative of the cement paste microstructure. Fig. 4 is representative of those parts of the C_3S paste where CH has not formed. As shown previously (Figs. 1 and 2), CH tended to concentrate entirely in certain areas and totally fill up large pore spaces, leaving other areas such as that depicted in Fig. 4 free of CH. As discussed in the preceding section, there seem to be close contact between residual anhydrous grains and product in the C_3S and alite sys-

tems. In these pastes, as C–S–H precipitates close to the C_3S surfaces largely as inner products, most of the capillary pore space is left open in those areas not occupied by CH.

C–S–H and CH is much more evenly distributed throughout the microstructure in the cement paste. This is, at least in part, a consequence of Hadley grain formation. As little product appear to form inside the peripheries of the original anhydrous grains in Portland cement paste at 24 h (cf. previous section and Figs. 3, 7 and 8), it has to form outside and causes thus considerable filling and densification of the capillary pore space. The commercially ground anhydrous cement appeared to contain a much higher number of submicrometer sized particles than did the laboratory-ground C_3S or alite, as seen in secondary electron mode SEM of the unhydrated cement and cement mineral samples. Scrivener [25] suggested that very small anhydrous grains form 'rosettes' of C–S–H when they react. It appears that the relatively continuous outer product phase (cf. Figs. 3, 7 and 8) is composed of clusters of such C–S–H rosettes, presumably filled in subsequently by reaction products resulting from the hydration of the larger cement grains. The difference in observed microstructure between the cement paste and the alite and C_3S pastes is not related to differences in extent of hydration. Image analysis showed the degree of hydration to be in the range 30–35% for all pastes examined after 24 h.

The outer product phase in the Portland cement paste has a fibrous character as seen from Figs. 7 and 8, very similar in appearance to that reported by Scrivener [25] from STEM and TEM studies of pastes of similar age. The more weakly defined C–S–H fibrils in the C_3S and alite pastes appear to stretch some 200 nm out in the capillary pore space (Fig. 5), and bears close similarities to outer product C–S–H as it appears in C_3S paste of similar age in TEM [8,31]. In agreement with the observation of Jennings and Parrott [5], an exact boundary between outer product and inner product was not clearly resolved in the C_3S and alite pastes at 24 h, as there is no consistent variation in morphology or brightness over the shell of C–S–H. The relatively weakly defined fibers stretching out in the capillary pore space is clearly outer product C–S–H, but it is less clear if a more substantial part of the hydration shell is also outer product C–S–H.

3.4. Distribution of C–S–H at 1 month

A range of low- to high-magnification images of the C_3S paste hydrated for 1 month are shown Figs. 2, 11 and 12. In areas outside those totally occupied by CH (cf. section on CH distribution) the capillary pore system is easily resolvable, and capillary pores up to several micrometers are common. Micrographs of the Portland cement paste hydrated for 1 month are depicted in Figs. 13 and 14, Fig. 14 showing a close-up of the framed area of Fig. 13. Figs. 11 and 12 of the C_3S system are of the same magnification as Figs. 13 and 14 of the cement paste, respectively, and suited for direct comparison. The overall microstructure of the C_3S paste is, as previously indicated, much simpler and appear more structured than that of the Portland cement. It appears to consist of a few characteristic features: CH deposits that have totally filled up capillary pore system in some areas, leaving other areas of the capillary pore system entirely free of CH; remnant C_3S cores surrounded by relatively homogeneous inner product C–S–H; large particles (>5 μm) of relatively homogeneous inner product C–S–H gel; and small grains (<5 μm) of inner product C–S–H of variable porosity. The inner product C–S–H is covered by a layer of brighter C–S–H (probably outer product C–S–H), with fibrous C–S–H radiating out in the open capillary pore space.

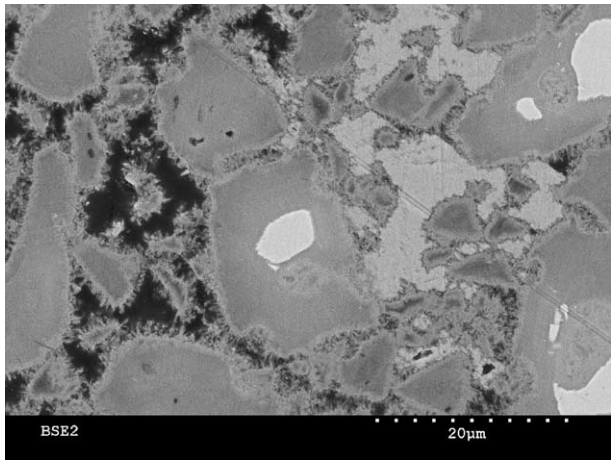

Fig. 12. Backscattered electron image (FE-SEM) of the C_3S paste hydrated for 1 month. Magnification: 2000×.

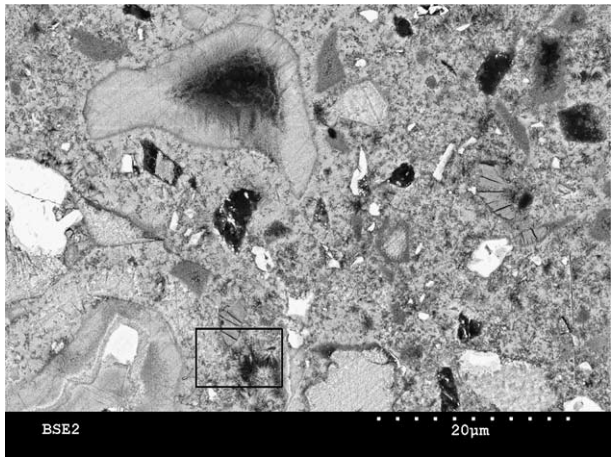

Fig. 13. Backscattered electron image (FE-SEM) of the cement paste hydrated for 1 month. Magnification: 2000×.

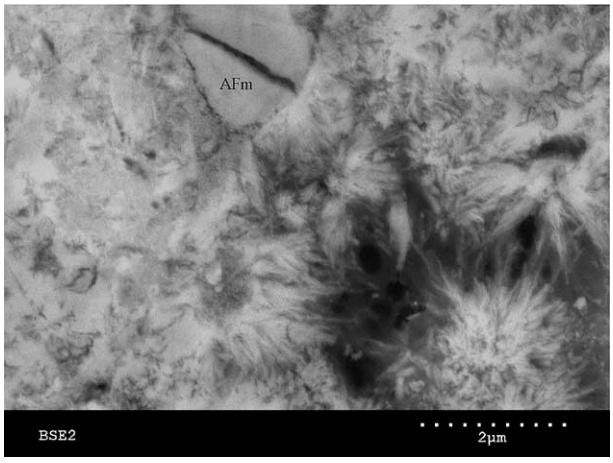

Fig. 14. Backscattered electron image (FE-SEM) of the cement paste hydrated for 1 month. Close-up of the area framed in Fig. 13. Magnification: 15,000×.

In contrast, the Portland cement paste consists of a large variety of different microstructural features including: finely dispersed CH; remnant ferrite and other cement particles; Hadley grains; inner product phases of C–S–H but with considerable variation in composition and porosity; and occasional monosulfate (AFm) deposits; all in a matrix material consisting of primarily C–S–H. At the w/c ratio of 0.40 used, capillary porosity is resolved only rarely; an example is seen at the lower right part of Fig. 14. An AFm particle is seen at the top of Fig. 14. In many areas there appears to be a relatively clear defined borderline between inner and outer products (Fig. 13), but the inner product phase (or phenograin structure according to the Bonen and Diamond [32] terminology) is not as homogeneous and featureless as that in the C_3S paste.

The high degree of homogeneity and fine-scale structure of inner product C–S–H in mature C_3S paste has also been observed in TEM [9]; this phase appear to constitute the bulk of the microstructure in the mature C_3S paste, in agreement with previous TEM observations [8,9]. While a groundmass structure [32] is apparent in the mature cement pastes, one can hardly speak of a groundmass structure in C_3S paste. CH dominates as groundmass material in those areas where CH prevails, while the capillary pores dominate the matrix in the other parts.

Generally speaking, the fibrous appearance of the outer product C–S–H becomes more developed at 1 month than at 24 h; this holds for both C_3S (Figs. 11 and 5) and cement (Figs. 7 and 14). Where space is available the length of the fibers appears to have increased, and fiber lengths up to about 700 nm are seen. The length and physical appearance of the fibrous outer product C–S–H is similar to what has been observed in TEM previously [8,10,30]. However, the fibrous C–S–H appears finer, or more sheet-like, in the TEM micrographs. This can be due the different types of specimens used (bulk vs. thin-sections), and to the different sources of contrast generation [11] making for the higher resolution in the TEM.

In the C_3S and alite pastes the fibrous outer product C–S–H extends out into the capillary pore space from a denser sub-layer. There is often a distinct border between this bright outer sub-layer and the darker interior C–S–H phase (Fig. 11). The structure resembles that observed in STEM/TEM of mature C_3S paste by Dalgleish et al. [7]. There are reasons to believe that the brighter sub-layer is outer product C–S–H, while the darker gray interior product is inner product C–S–H. This view is substantiated by the observation that the fibrous product and brighter sub-layer are found around practically all hydrated grains, and also around the small fully hydrated grains. The bright sub-layer developed after the hydration of the small C_3S grains, and therefore must have precipitated from the initially water-filled space (i.e. as outer product). This feature should not be confused with the two-tone structure of the inner product C–S–H observed in mature alite paste [5] and in Portland cement systems [33–35].

4. Conclusions

The FE-SEM adopted in this study provided micrographs of higher resolution than those previously obtained from backscattered electron mode studies of cement and concrete. The resolution is still less than, but approaches that used in many TEM studies. As the thinned-sections used in TEM, and the polished bulk specimens used in SEM, are both cross-sectional representations of the microstructure, comparisons of features can be made. This FE-SEM study reveals similar microstructural details as seen in TEM of ion-thinned sections. Previous findings in the TEM of featureless inner product C–S–H phases, fibrous outer product C–S–H phases and small 'fully hydrated grains' are also observed from backscattered electron mode FE-SEM. These features are found in the present FE-SEM examinations of Portland cement paste and in C_3S and alite pastes as well. While polished sections without noticeable artifacts can be difficult to obtain for standard backscattered electron mode SEM [14], it is clear that high-resolution studies requires an even higher degree of perfection in the art of specimen preparation. This study shows it is possible to obtain polished specimens suited for high-resolution backscattered electron mode SEM by use of established preparation techniques [14].

The microstructures of the C_3S and alite pastes examined were very similar; the microstructure of the Portland cement paste differed in many respects from

them. The mature C_3S and alite pastes displayed only of a few characteristic features:

- CH that had totally filled up the capillary pore system in enclosed but large spaces, leaving other parts of the capillary pore system open and free of CH.
- Large (>5 μm) and relatively homogeneous areas of inner product C–S–H, some with remnant C_3S cores.
- Small (<5 μm) relict C_3S grains consisting of inner product C–S–H of highly variable porosity.
- A thin boundary layer of brighter C–S–H (probably outer product C–S–H), with fibrous C–S–H radiating out in the open capillary pore space.

The Portland cement paste microstructure was much more complex, and contained a large variety of different microstructural features including; monosulfate (AFm), finely dispersed CH, remnant ferrite and other cement particles, Hadley grains, and inner product C–S–H of variable composition and porosity, in a matrix of undesignated character but consisting primarily of C–S–H. Capillary porosity was resolved only rarely in the mature Portland cement paste at 0.40 water/cement ratio.

Hollow shells, or Hadley grains, were observed in both the C_3S and alite pastes at 24 h. This observation challenges previous claims that C_3S alone do not hydrate so as to leave Hadley grains. The hollow shells appeared to be produced from the rapid early hydration of the small C_3S particles (<5 μm) only. The center of the Hadley grains appeared to be hollowed, and gapped Hadley grains with remnant unreacted C_3S cores were rarely seen. There was contact between shell of C–S–H and remnant C_3S cores. While hollow-shell grains appeared to be limited to the small grains in the C_3S and alite pastes, they were also seen in the larger cement grains in the Portland cement paste (primarily as gapped Hadley grains with a remnant cement core). Thus, a mode of hydration leading to hollow-shell grains seems to occur in both C_3S and Portland cement systems.

References

[1] Diamon M, Ueda S, Kondo R. Morphological study of hydration of tricalcium silicate. Cem Concr Res 1971;1(4):391–401.

[2] Williamson RB. Solidification of Portland cement. Progr Mater Sci 1972;15:189–286.

[3] Lawrence FV, Young JF. Studies on the hydration of tricalcium silicate pastes I. Scanning electron microscopic examination of microstructural features. Cem Concr Res 1973;3(2):149–61.

[4] Goto S, Daimon M, Hosaka G, Kondo R. Composition and morphology of hydrated tricalcium silicate. J Am Ceram Soc 1976;59(7–8):281–4.

[5] Jennings HM, Parrott LJ. Microstructural analysis of hydrated alite paste Part 2: Microscopy and reaction products. J Mater Sci 1986;21:4053–9.

[6] Diamond S. Aspects of concrete porosity revisited. Cem Concr Res 1999;29:1181–8.

[7] Dalgleish BJ, Pratt PL, Moss RI. Preparation techniques and the microscopical examination of Portland cement paste and C_3S. Cem Concr Res 1980;10(5):665–76.

[8] Jennings HM, Dalgleish BJ, Pratt PL. Morphological development of hydrating tricalcium silicate as examined by electron microscopy techniques. J Am Ceram Soc 1981;64(10):567–72.

[9] Growes GW, Le Sueur PJ, Sinclair W. Transmission electron microscopy and microanalytical studies of ion-beam-thinned sections of tricalcium silicate paste. J Am Ceram Soc 1986;69(4):353–6.

[10] Richardson IG. The nature of C–S–H in hardened cement. Cem Concr Res 1999;29:1131–47.

[11] Richardson IG. Electron microscopy of cements. In: Bensted J, Barnes P, editors. Structure and performance of cements. London: Spon Press; 2002. p. 500–56.

[12] Kjellsen KO, Lagerblad B, Jennings HM. Hollow-shell formation—an important mode in the hydration of Portland cement. J Mater Sci 1997;32:2921–7.

[13] Kjellsen KO, Wallevik OH, Hallgren M. On the compressive strength development of high-performance concrete and paste-effect of silica fume. Mater Struct 1999;32(1):63–9.

[14] Kjellsen KO, Monsøy A, Isachsen K, Detwiler RJ. Preparation of flat-polished specimens for SEM-backscattered electron imaging and X-ray microanalysis—importance of epoxy impregnation. Cem Concr Res 2003;33:611–6.

[15] Verbeck G. Pore structure. Bulletin 197, PCA Research and Development Laboratories, Skokie, Portland Cement Association, 1966.

[16] Berger RL, McGregor JD. Influence of calcium hydroxide formed during tricalcium silicate hydration. Cem Concr Res 1972;2:43–55.

[17] Berger RL, McGregor JD. Effect of temperature and water–solid ratio on growth of $Ca(OH)_2$ crystals formed during hydration of Ca_3SiO_5. J Am Ceram Soc 1973;56(2):73–9.

[18] Boyer JP, Berger RL. Influence of temperature increases during the induction period of C_3S hydration on the microstructure and strength of C_3S mortars. J Am Ceram Soc 1980;63:675–80.

[19] Diamond S. Calcium hydroxide in cement paste and concrete—a microstructural appraisal. In: Skalny J, Gebauer J, Odler I, editors. Materials science of concrete, Special Volume: calcium hydroxide in concrete. Westerville: The American Ceramic Society; 2001. p. 37–58.

[20] Taplin JH. A method for following the hydration reaction in Portland cement. Austr J Appl Sci 1959;10:329–45.

[21] Hadley DW. The nature of the paste-aggregate interface. PhD thesis, West Lafayette, Purdue University, 1972.

[22] Barnes BD, Diamond S, Dolch WL. Hollow shell hydration of cement particles in bulk cement paste. Cem Concr Res 1978;8(3):263–72.

[23] Dalgleish BJ, Pratt PL, Toulson E. Fractographic studies of microstructural development in hydrated Portland cement. J Mater Sci 1982;17:2199–207.

[24] Pratt PL, Ghose A. Electron microscope studies of Portland cement microstructures during setting and hardening. Phil Trans R Soc Lond 1983;A310:93–103.

[25] Scrivener KL. The microstructure of concrete. In: Skalny J, editor. Materials science of concrete, vol. 1. Westerville: The American Ceramic Society; 1989. p. 127–61.

[26] Kjellsen KO, Jennings HM, Lagerblad B. Evidence of hollow shells in the microstructure of cement paste. Cem Concr Res 1996;26(4):593–9.

[27] Hadley DW, Dolch WL, Diamond S. On the occurrence of hollow-shell hydration grains in hydrated cement paste. Cem Concr Res 2000;30(1):1–6.

[28] Taylor HFW et al. The hydration of tricalcium silicate. Report RILEM Technical Committee 68-MMH. Mater Struct 1984;17(102):457–68.
[29] Scrivener KL, Pratt PL. Microstructural studies of the hydration of C_3A and C_4AF independently and in cement paste. In: Glasser FP, editor. British Ceramic Proceedings No 35 Stoke-on-Trent. British Ceramic Society; 1984. p. 207–19.
[30] Richardson IG, Groves GW. Microstructure and microanalysis of hardened ordinary Portland cement. J Mater Sci 1993;28:265–77.
[31] Henderson E, Bailey JE. The compositional and molecular character of the calcium silicate hydrates formed in the paste hydration of $3CaO \cdot SiO_2$. J Mater Sci 1993;28:3681–91.
[32] Bonen D, Diamond S. Interpretation of compositional patterns found by quantitative energy dispersive X-ray analysis for cement paste constituents. J Am Ceram Soc 1994;77(7):1875–82.
[33] Scrivener KL. The effect of heat treatment on inner product C–S–H. Cem Concr Res 1992;22:1224–6.
[34] Diamond S, Olek J, Wang Y. The occurrence of two-tone structures in room-temperature cured cement paste. Cem Concr Res 1998;28(9):1237–43.
[35] Famy C, Scrivener KL, Crumbie AK. What causes differences of C–S–H gel grey levels in backscattered electron images? Cem Concr Res 2002;32:1465–71.